

1 Soil Moisture and Hydrology Projections of the Permafrost 2 Region: A Model Intercomparison

3 Christian G. Andresen^{1,2}, David M. Lawrence³, Cathy J. Wilson¹, A. David McGuire⁴, Charles
4 Koven⁵, Kevin Schaefer⁶, Elchin Jafarov^{6,1}, Shushi Peng⁷, Xiaodong Chen⁸, Isabelle
5 Gouttevin^{9,10}, Eleanor Burke¹¹, Sarah Chadburn¹², Duoying Ji¹³, Guangsheng Chen¹⁴, Daniel
6 Hayes¹⁵, Wenxin Zhang^{16,17}

7
8 ¹Earth and Environmental Science Division, Los Alamos National Laboratory, Los Alamos, New Mexico, USA

9 ²Geography Department, University of Wisconsin Madison, Madison, Wisconsin, USA

10 ³National Center for Atmospheric Research, Boulder, Colorado, USA

11 ⁴Institute of Arctic Biology, University of Alaska Fairbanks, Fairbanks, Alaska, USA

12 ⁵Climate and Ecosystem Sciences Division, Lawrence Berkeley National Lab, Berkeley, CA, USA

13 ⁶Institute of Arctic Alpine Research, University of Colorado Boulder, Boulder, Colorado, USA

14 ⁷UJF–Grenoble 1/CNRS, Laboratoire de Glaciologie et Géophysique de l'Environnement (LGGE), Grenoble, France

15 ⁸Department of Civil and Environmental Engineering, University of Washington, Seattle, Washington, USA

16 ⁹IRSTEA-HHLY, Lyon, France.

17 ¹⁰IRSTEA-ETNA, Grenoble, France.

18 ¹¹Met Office Hadley Centre, UK

19 ¹²School of Earth and Environment, University of Leeds, UK

20 ¹³College of Global Change and Earth System Science, Beijing Normal University, China

21 ¹⁴Environmental Sciences Division, Oak Ridge National Laboratory, Oak Ridge, Tennessee, USA

22 ¹⁵ School of Forest Resources, University of Maine, Maine, USA

23 ¹⁶ Department of Physical Geography and Ecosystem Science, Lund University, Lund, Sweden

24 ¹⁷Center for Permafrost (CENPERM), Department of Geosciences and Natural Resource Management, University of
25 Copenhagen, Denmark

26
27 *Correspondence to:* Christian G. Andresen (candresen@wisc.edu)

28
29 **Abstract.** This study investigates and compares soil moisture and hydrology projections of broadly-used
30 land models with permafrost processes and highlights the causes and impacts of permafrost zone soil
31 moisture projections. Climate models project warmer temperatures and increases in precipitation (P)
32 which will intensify evapotranspiration (ET) and runoff in land models. However, this study shows that
33 most models project a long-term drying of the surface soil (0-20cm) for the permafrost region despite
34 increases in the net air-surface water flux (P-ET). Drying is generally explained by infiltration of moisture
35 to deeper soil layers as the active layer deepens or permafrost thaws completely. Although most models
36 agree on drying, the projections vary strongly in magnitude and spatial pattern. Land-models tend to agree
37 with decadal runoff trends but underestimate runoff volume when compared to gauge data across the
38 major Arctic river basins, potentially indicating model structural limitations. Coordinated efforts to
39 address the ongoing challenges presented in this study will help reduce uncertainty in our capability to
40 predict the future Arctic hydrological state and associated land-atmosphere biogeochemical processes
41 across spatial and temporal scales.

42 43 1. Introduction

44
45 Hydrology plays a fundamental role in permafrost landscapes by modulating complex interactions among
46 biogeochemical cycling (Frey and McClelland, 2009; Newman et al., 2015; Throckmorton et al., 2015),
47 geomorphology (Grosse et al., 2013; Kanevskiy et al., 2017; Lara et al., 2015; Liljedahl et al., 2016) and
48 ecosystem structure and function (Andresen et al., 2017; Avis et al., 2011; Oberbauer et al., 2007).
49 Permafrost has a strong influence on hydrology by controlling surface and sub-surface distribution,

50 storage, drainage and routing of water. Permafrost prevents vertical water flow which often leads to
51 saturated soil conditions in continuous permafrost while confining subsurface flow through perennially-
52 unfrozen zones (a.k.a. taliks) in discontinuous permafrost (Jafarov et al., 2018; Walvoord and Kurylyk,
53 2016). However, with the observed (Streletskiy et al., 2008) and predicted (Slater and Lawrence, 2013)
54 thawing of permafrost, there is a large uncertainty in the future hydrological state of permafrost
55 landscapes and in the associated responses such as the permafrost carbon-climate feedback.

56 The timing and magnitude of the permafrost carbon-climate feedback is, in part, governed by changes in
57 surface hydrology, through the regulation by soil moisture of the form of carbon emissions from thawing
58 labile soils and microbial decomposition as either CO₂ or CH₄ (Koven et al., 2015; Schädel et al., 2016;
59 Schaefer et al., 2011). The impact of soil moisture changes on the permafrost-carbon feedback could be
60 significant. Lawrence et al. (2015) found that the impact of the soil drying projected in simulations with
61 the Community Land Model decreased the overall Global Warming Potential of the permafrost carbon-
62 climate feedback by 50%. This decrease was attributed to a much slower increase in CH₄ emissions if
63 surface soils dry, which is partially compensated for by a stronger increase in CO₂ emissions under drier
64 soil conditions.

65 Earth System Models project an intensification of the hydrological cycle characterized by a general
66 increase in the magnitude of water fluxes (e.g. precipitation, evapotranspiration and runoff) in northern
67 latitudes (Rawlins et al., 2010; Swenson et al., 2012). In addition, intensification of the hydrological cycle
68 is likely to modify the spatial and temporal patterns of water in the landscape. However, the spatial
69 variability, timing, and reasons for future changes in hydrology in terrestrial landscapes in the Arctic are
70 unclear and variability in projections of these features by current terrestrial hydrology applied in the
71 Arctic have not been well documented. Therefore, there is an urgent need to assess and better understand
72 hydrology simulations in land models and how differences in process representation affect projections of
73 permafrost landscapes.

74 Upgrades in permafrost representation such as freeze and thaw processes in the land component of Earth
75 System Models have improved understanding of the evolution of hydrology in high northern latitudes.
76 Particularly, soil thermal dynamics and active layer hydrology upgrades include the effects of unfrozen
77 water on phase change, insulation by snow (Peng et al., 2015), organic soils (Jafarov, E. and Schaefer,
78 2016; Lawrence et al., 2008) and cold region hydrology (Swenson et al., 2012). Nonetheless, large
79 discrepancies in projections remain as the current generation of models substantially differ in soil thermal
80 dynamics (e.g. Peng *et al* 2015, Wang *et al* 2016). In particular, variability among current models
81 simulations of the impact of permafrost thaw on soil water and hydrological states is not well
82 documented. Therefore, in this study we analyze the output of a collection of widely-used “permafrost-
83 enabled” land models. These models participated in the Permafrost Carbon Network Model
84 Intercomparison Project (PCN-MIP) (McGuire et al., 2018, 2016) and contained the state-of-the art
85 representations of soil thermal dynamics in high latitudes at that time. In particular, we assess how
86 changes in active layer thickness and permafrost thaw influence near-surface soil moisture and hydrology
87 projections under climate change. In addition, we provide comments on the main gaps and challenges in
88 permafrost hydrology simulations and highlight the potential implications for the permafrost carbon-
89 climate feedback.

90
91
92
93

94 2. Methods

95

96 2.1 Models and Simulation Protocol

97

98 This study assesses a collection of terrestrial simulations from models that participated in the PCN-MIP
99 (McGuire et al., 2018, 2016) (Table 1). The analysis presented here is unique as it focuses on the
100 hydrological component of these models. Table 2 describes the main hydrological characteristics for each
101 model. Additional details on participating models regarding soil thermal properties, snow, soil carbon and
102 forcing trends can be found in previous PCN-MIP studies (e.g. McGuire *et al* 2016, Koven *et al* 2015,
103 Wang *et al* 2016, Peng *et al* 2015). It is important to note that the versions of the models presented in this
104 study are from McGuire *et al* (2016, 2018) and some additional improvements to individual models may
105 have been made since then.

106 The simulation protocol is described in detail in *McGuire et al.*, (2016, 2018). In brief, models'
107 simulations were conducted from 1960 to 2299, partitioned by an historic (1960-2009) and future
108 simulation (2010-2299), forced with a common projected climate derived from a fully coupled climate
109 model simulation (CCSM4) (Gent et al., 2011). Historic atmospheric forcing datasets (Table 1) (e.g.
110 climate, atmospheric CO₂, N deposition, disturbance, etc.) and spin-up time were specific to each
111 modeling group. The horizontal resolution (0.5° – 1.25°) and soil hydrological column configurations
112 (depths ranging from 2 to 47m and 3 to 30 soil layers) also vary across models (Figure 1). We focus on
113 results from simulations forced with climate and CO₂ from the Representative Concentration Pathway
114 (RCP) 8.5 scenario, which represents unmitigated, “business as usual” emissions of greenhouse gases.
115 Future simulations were calculated from monthly climate anomalies for the Representative Concentration
116 Pathway (RCP 8.5, 2006-2100) and the Extension Concentration Pathway (ECP 8.5, 2101-2299)
117 scenarios overlaid by repeating historic forcing atmospheric datasets from CCSM4 (Gent et al., 2011).

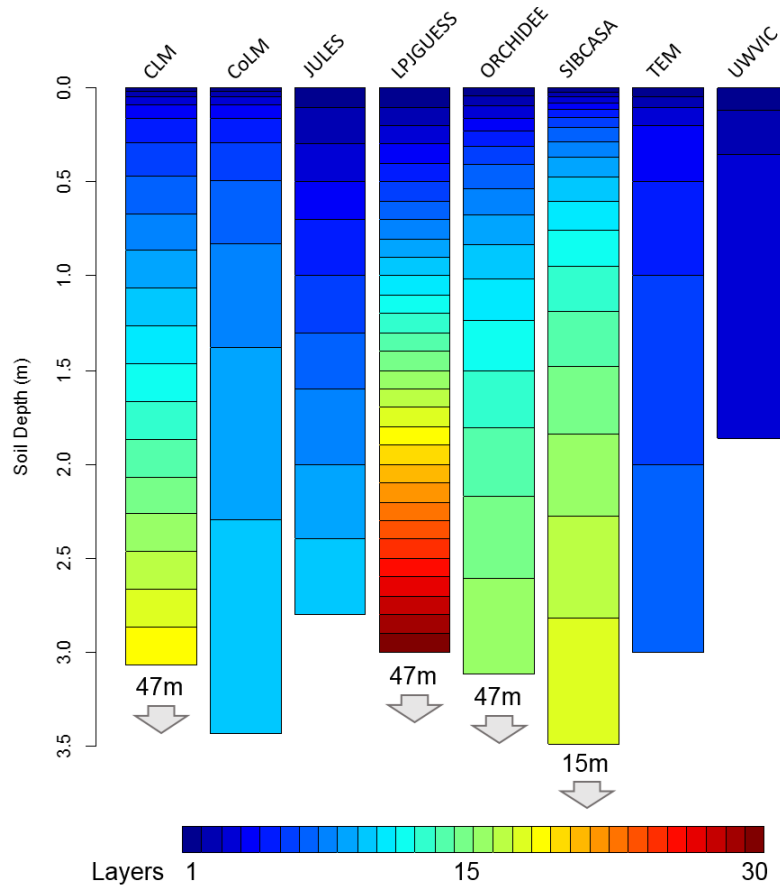
118

119 2.2 Permafrost and Hydrology Variables Analyzed

120

121 Our analysis focused on the permafrost regions in the Northern Hemisphere north of 45°N. This
122 qualitative hydrology comparison was based on the full permafrost domain for each model rather than a
123 common subset among models in order to fully portray the overall changes in permafrost hydrology for
124 participating models. For each model, we define a grid cell as containing near-surface permafrost if the
125 annual monthly maximum active layer thickness (ALT) is at or less than the 3m depth layer depending on
126 the model soil configuration (Figure 1) (McGuire et al., 2016; Slater and Lawrence, 2013). Participating
127 models represent frozen soil for layers with temperature of <273.15°k, acting as an impermeable layer for
128 liquid water. We assessed how permafrost changes affect near-surface soil moisture, defined here as the
129 soil water content (kg/m²) of the 0-20 cm soil layer. We focused on the top 20 cm of the soil column due
130 to its relevance to near-surface biogeochemical processes. We added the weighted fractions for each
131 depth interval to calculate near-surface soil moisture (0-20cm) to account for the differences in the
132 vertical resolution of the soil grid cells among models (Figure 1). To better understand the causes and
133 consequences of changes in soil moisture, we examined several principal hydrology variables including
134 evapotranspiration (ET), runoff (R; surface and sub-surface) and precipitation (P; snow and rain).
135 Representation of ET, R and soil hydrology varies across participating models and are summarized in
136 table 2.

137 We compared model simulations with long-term (1970-1999) mean monthly discharge data from Dai *et al*
 138 2009. We computed model mean annual discharge including surface and subsurface runoff for the main
 139 river basins in the permafrost region of North America (Mackenzie, Yukon) and Russia (Yenisei, Lena).
 140 Gauge stations from major permafrost river basins used for simulation comparison include (i) Arctic Red,
 141 Canada (67.46°N, 133.74°W) for Mackenzie River, (ii) Pilot Station, Alaska (61.93°N 162.88°W) for
 142 Yukon River, (iii) Igarka, Russia (67.43°N, 86.48°E) for Yenisey River and (iv) Kusur, Russia (70.68°N,
 143 127.39°E) for Lena River.
 144



145
 146
 147 **Figure 1. Soil hydrologically-active column configuration for each participating model. Numbers**
 148 **and arrows indicate full soil configuration of non-hydrologically active bedrock layers. Colors**
 149 **represent the number of layers.**

150
 151
 152 **Table 1. Models description and driving datasets.**

Model	Full Name	Climate Forcing Dataset	Model Reference	Short-Wave radiation ^a	Long-Wave Radiation ^a	Vapor Pressure ^a
CLM 4.5	Community Land Model v4.5	CRUNCEP4 ^b	Oleson <i>et al</i> (2013)	Yes	Yes ^c	Yes

CoLM	Common Land Model	Princeton ^d	Dai <i>et al</i> (2003), Ji <i>et al</i> (2014)	Yes	Yes	Yes
JULES	Joint UK Land Environment Simulator model	WATCH (1901-2001) ^e	Best <i>et al</i> (2011)	Yes	Yes	Yes
ORCHIDEE-IPSL	Organising Carbon and Hydrology In Dynamic Ecosystems	WATCH (1901-1978) ^e	Gouttevin, I. <i>et al</i> (2012), Koven <i>et al</i> (2009), Krinner <i>et al</i> (2005)	Yes	Yes	Yes
LPJGUESS	Lund-Postdam-Jena dynamic global veg model	CRU TS 3.1 ^f	Gerten <i>et al</i> (2004), Wania <i>et al</i> (2009b, 2009a)	Yes	No	No
SiBCASA	Simple Biosphere/Carnegie-Ames-Stanford Approach model	CRUNCEP4 ^b	Schaefer <i>et al</i> (2011), Bonan (1996), Jafarov, E. and Schaefer (2016)	Yes	Yes	Yes
TEM604	Terrestrial Ecosystem Model	CRUNCEP4 ^b	Hayes <i>et al</i> (2014, 2011)	Yes	No	No
UW-VIC	Univ. of Washington Variable Infiltration Capacity model	CRU ^f , Udel ^h	Bohn <i>et al</i> (2013)	Internally calculated	Internally calculated	Yes

^aSimulations driven by temporal variability

^bViovy and Ciais (<http://dods.extra.cea.fr/>)

^cLong-wave dataset not from CRUNCEP4

^dSheffield *et al* (2006) (<http://hydrology.princeton.edu/data.pgf.php>)

^ehttp://www.eu-watch.org/gfx_content/documents/README-WFDEI.pdf

^fHarris *et al* (2014), University of East Anglia Climate Research Unit (2013)

^gMitchell and Jones (2005) for temperature

^hWillmott and Matsuura (2001) for wind speed and precipitation with corrections (see Bohn *et al.* 2013).

153 **Table 2. Hydrology and soil thermal characteristics of participating models.**

Model	Hydrology								Soil Thermal Properties			
	Evapotranspiration approach	Root water uptake	Infiltration	Water table	Soil Water Storage and Transmission	Groundwater Dynamics	Soil-ice impact	Snow	Soil thermal dynamics approach	Unfrozen Water effects on Phase Change	Moss insulation	Organic soil insulation
CLM 4.5	Sum of canopy evaporation, transpiration, and soil evaporation	Macroscopic approach	Saturation-excess runoff $F_{sat}=f(z_{wt})$	Niu et al. (2007); perched water table possible if ice layer present	Richard's equation (Clapp Hornberger functions)	Base flow from TOPMODEL concepts, unconfined aquifer (Niu et al. 2007)	Impacts hydrologic properties through power-law ice impedance (Swenson et al., 2012)	Multi-layer dynamic (5 max)	Multi-layer Finite Difference Heat Diffusion	Yes	No	Yes
CoLM	BATS and Philip's (1957)	Macroscopic approach	Saturation-excess runoff $F_{sat}=f(z_{wt})$	Simple TOPMODEL	Richard's equation (Clapp Hornberger functions)	Base flow from TOPMODEL	Impacts hydrologic properties through power-law ice impedance	Multi-layer dynamic (5 max)	Multi-layer Finite Difference Heat Diffusion	No	No	No
JULES	Sum of ET, soil evaporation and moisture storages (e.g. lakes, urban) minus surface resistance	Macroscopic approach	Saturation-excess runoff $F_{sat}=f(z_{wt})$ or $F_{sat}=f(\theta)$	TOPMODEL or Probability Distribution Model	Richard's equation (Clapp Hornberger/van Genuchten functions)	Base flow from TOPMODEL	Hydraulic conductivity and suction determined by unfrozen water content (Brooks and Corey functions)	Multi-layer dynamic (3 max)	Multi-layer Finite Difference Heat Diffusion	Yes	No	No
ORCHIDEE-IPSL	Sum of bare soil, interception loss and plant transpiration for different veg PFTs in grid cell.	Macroscopic approach, water uptake different among cell veg PFTs (de Rosnay and Polcher, 1998)	Saturation-excess runoff $F_{sat}=f(\theta)$	TOPMODEL	Richard's equation (van Genuchten functions)	None	"Drying=Freezing" approximation (Gouttevin et al 2012)	Multi-layer dynamic (7 max)	1D Fourier Solution	Yes	No	Yes
LPJ-GUESS	Sum of Interception loss, plant transpiration and evaporation from soil. Gerten et al (2004)	Fractional water uptake from different soil layers according to prescribed root distribution. (Wania et al., 2009a,b)	Depends on soil moisture and layer thickness. Declines exponentially with soil moisture	Uniform, and only for wetland grid cell (Wania et al., 2009a,b)	Analog to Darcy's Law, percolation rate depends on soil texture conductivity and soil wetness (Haxelmeier and Prentice, 1996).	Base flow is based on the exponential function to estimate percolation rate	Impacts hydrologic properties through power-law ice impedance	Multi-layer dynamic (3 max)	Multi-layer Finite Difference Heat Diffusion	No	No	No
SIBCASA	Sum of ground evaporation, surface dew, canopy ET and canopy dew (Bonan, 1996)	Macroscopic approach	Infiltration approach in non-saturated porous media described by Darcy's law	Niu et al. (2007); perched water table possible if ice layer present	Richard's equation (Clapp Hornberger functions)	Base flow from TOPMODEL concepts, unconfined aquifer (Niu et al. 2007)	Impacts hydrologic properties through power-law ice impedance	Multi-layer dynamic (5 max)	Multi-layer Finite Difference Heat Diffusion	Yes	No	Yes
TEM-604	Jenson-Haise potential ET (PET, Jenson and Haise 1963). Actual ET is calculated based on PET, water availability and leaf mass.	Based on the proportion of actual ET to potential ET	Field capacity-excess runoff (Thornthwaite and Mather 1957)	none	one-layer bucket	none	none	Multi-layer dynamic (9 max)	Multi-layer Finite Difference Heat Diffusion	No	Yes	No
UW-VIC	Sum of canopy interception, veg. transpiration and soil evaporation (Liang et al. 1994)	Based on reference ET and soil wilting point	Saturation-excess runoff $F_{sat}=f(\theta)$	Microtopography	From infiltration rate and infiltration shape parameter (Liang et al. 1994). No lateral flow between model grids	Base flow from Arno model conceptualization (Francini and Pacciani 1991)	Impacts hydrologic properties through power-law ice impedance	Bulk-layer dynamic (2 max)	Multi-layer Finite Difference Solution	Yes	No	Yes

154

155

156 2. Results

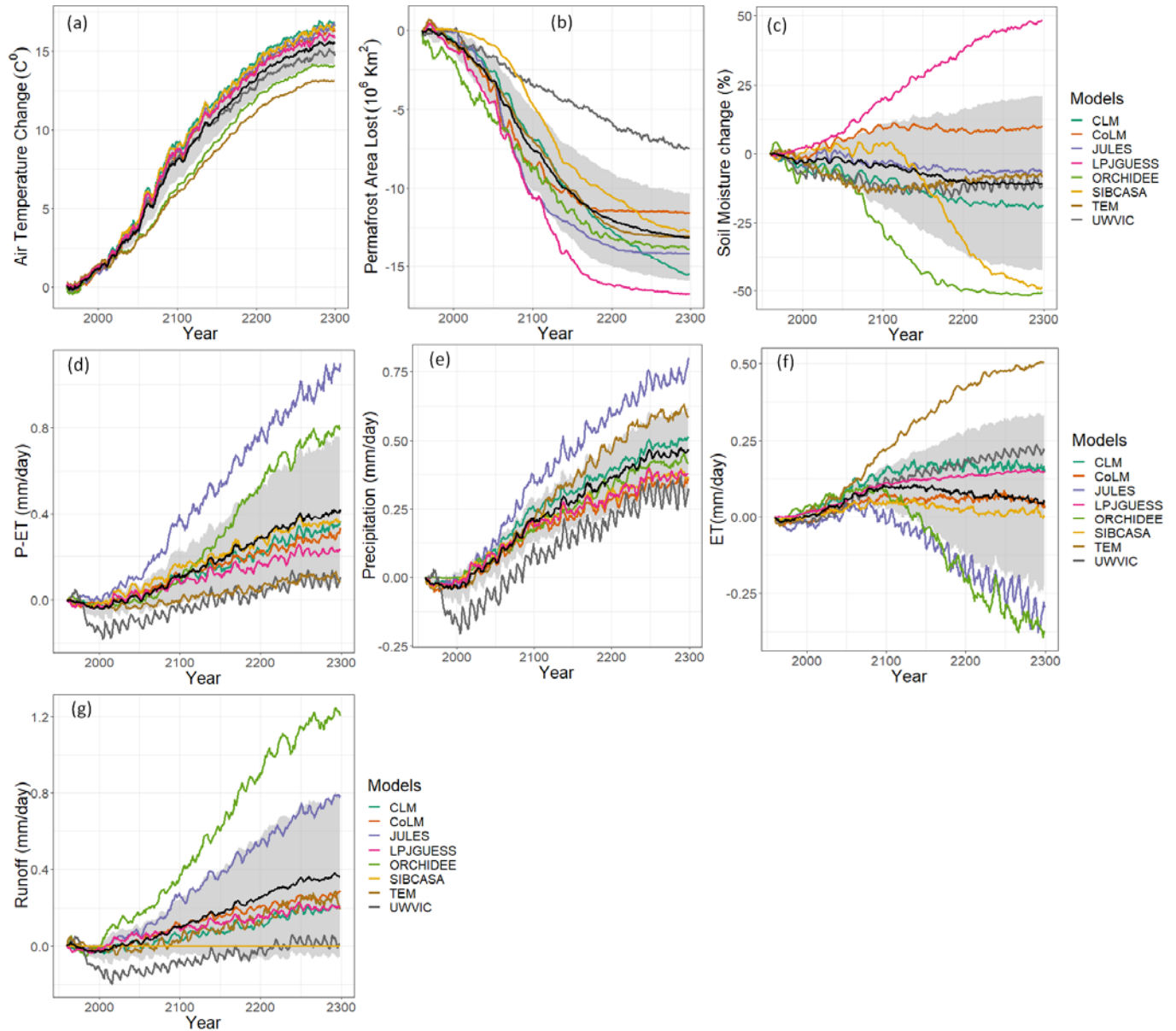
157

158 3.1 Soil Moisture

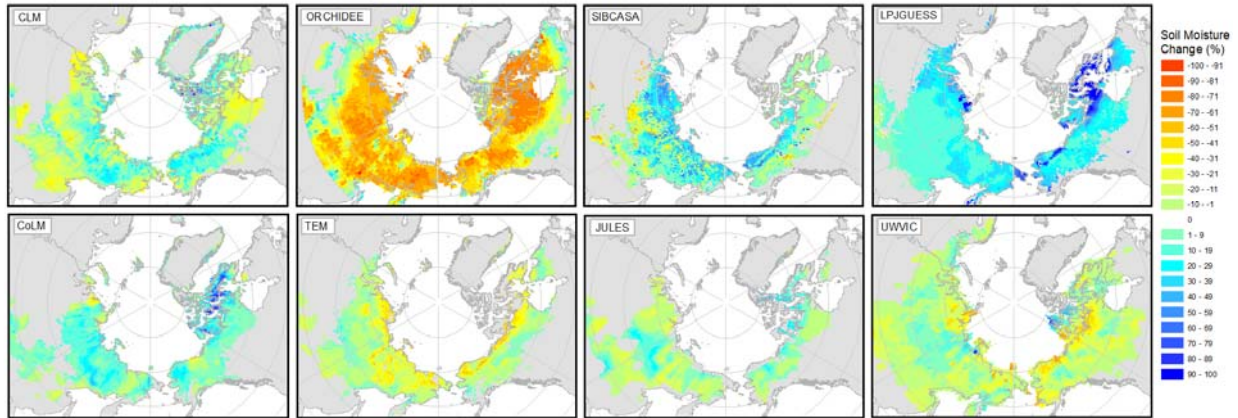
159

160 Air temperature forcing from greenhouse-gas emissions shows an increase of $\sim 15^{\circ}\text{C}$ in the permafrost
161 domain over the simulation period (Figure 2a). With increases in air temperature, models project an
162 ensemble mean decrease of ~ 13 million km^2 (91%) of the permafrost domain by 2299 (Figure 2b).
163 Coincident with these changes, most models projected a long-term drying of the near-surface soils when
164 averaged over the permafrost landscape (Figure 2c). However, the simulations diverged greatly with
165 respect to both the permafrost-domain average soil moisture response and their associated spatial patterns
166 (Figure 2c, 3). The models' ensemble mean indicated a change of -10% in near-surface soil moisture for
167 the permafrost region by year 2299, but the spread across models was large. COLM and LPJGUESS
168 simulate an increase in soil moisture of 10% and 48%, respectively. CLM, JULES, TEM6 and UWVIC
169 exhibit qualitatively similar decreasing trends in soil moisture ranging between -5% and -20%. SIBCASA
170 and ORCHIDEE projected a large soil moisture change of approximately -50% by 2299. Spatially,

171 models show diverse wetting and drying patterns and magnitudes across the permafrost zone (Figure 3).
 172 Several models tend to get wetter in the colder northern permafrost zones and are more susceptible to
 173 drying along the southern permafrost margin. Other models, such as TEM6 and UWVIC show the
 174 opposite pattern with drying more common in the northern part of the permafrost domain.
 175



176
 177 **Figure 2. Simulated annual mean changes in air temperature, near-surface permafrost area, near-**
 178 **surface soil moisture and hydrology variables relative to 1960 (RCP 8.5). Annual mean is computed**
 179 **from monthly output values. The black line represents the models' ensemble mean and the gray**
 180 **area is the ensemble standard deviation. Figures d, e, f, and g are represented as change from 1960**
 181 **values. Time series are smoothed with a 7-year running mean and calculated over the initial**
 182 **permafrost domain of each model in 1960 for latitude >45°N.**
 183
 184



185
186
187
188
189
190

Figure 3. Spatial variability of projected changes in surface soil moisture (%) among models. Depicted changes are calculated as the difference between the 2071 to 2100 average and the 1960 to 1989 average. Colored area represents the initial simulated permafrost domain of 1960 for each model.

191

3.2 Drivers of Soil Moisture Change

192

193

194

195

196

197

198

199

200

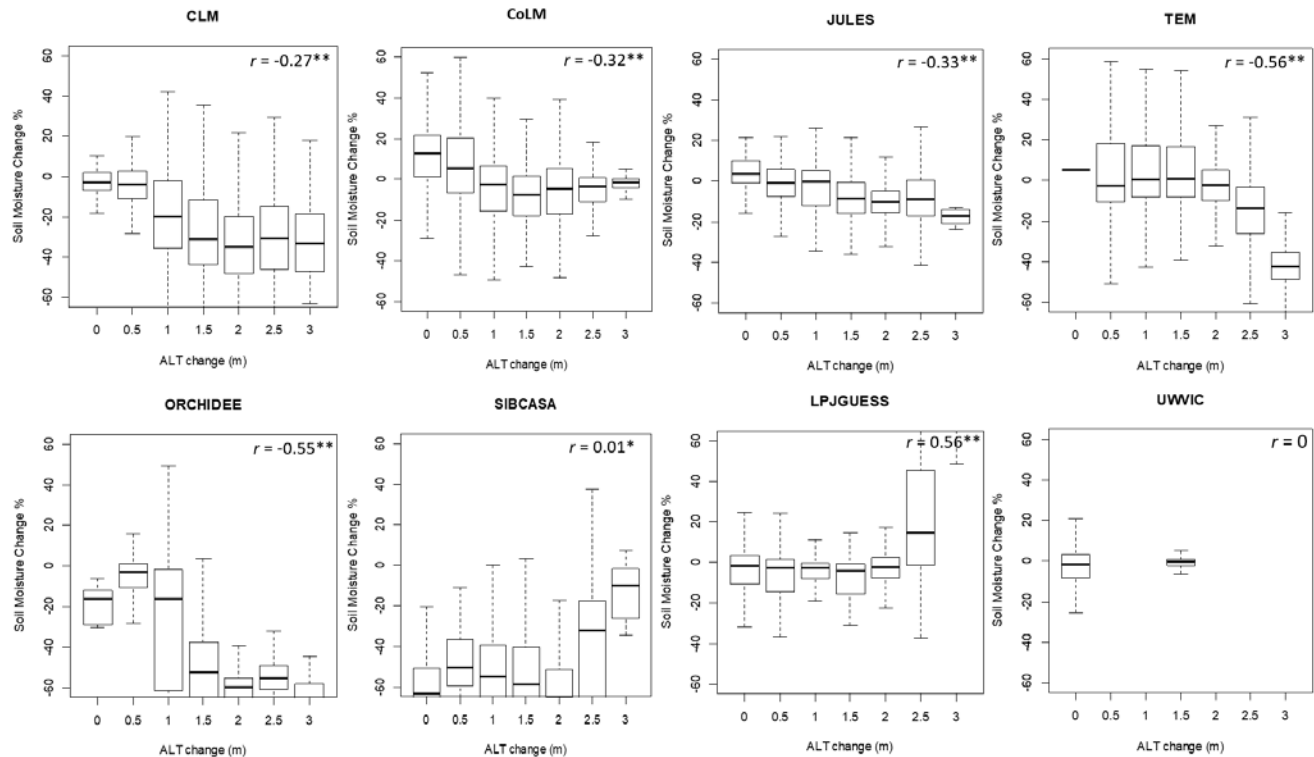
201

202

203

204

To understand why models projected upper soil drying despite increases in the net precipitation (P-ET) into the soil, we examined whether or not increases in active layer thickness (ALT) and/or complete thaw of near-surface permafrost could be related to surface soil drying of the top 0-20cm ALT. We observed a general significant negative trend in most models, except SIBCASA, LPJGUESS and UWVIC, where cells with greater increases in active layer thickness have greater drying (decrease) in near-surface soil moisture (Figure 4). However, there is a large spread between soil moisture and ALT changes (Figure 4). This spread may be influenced by many interacting factors that can be difficult to assess directly and are out of the scope of this study. In addition, the coarse soil column discretization in UWVIC limited this analysis for this model (Figure 1). However, most models show some indication that as the active layer deepens, soils tend to get drier at the surface.



205
206

207 **Figure 4. Responses of August near-surface (0-20cm) soil moisture to ALT changes. Each box**
 208 **represents a range of ± 0.25 m of ALT change. ALT and soil moisture change are calculated as the**
 209 **2290-2299 average minus the 1960-1989 average for cells in the initial permafrost domain of 1960.**
 210 **For cells where ALT exceeded 3 meters (no permafrost) during 2270-2299 period, we subtracted**
 211 **the initial active layer thickness (1960-1989 average) to 3 meters. Pearson correlations (r)**
 212 **significant at $*p < 0.01$ and $**p < 2e-16$.**
 213

214 3.3 Precipitation, ET, and Runoff

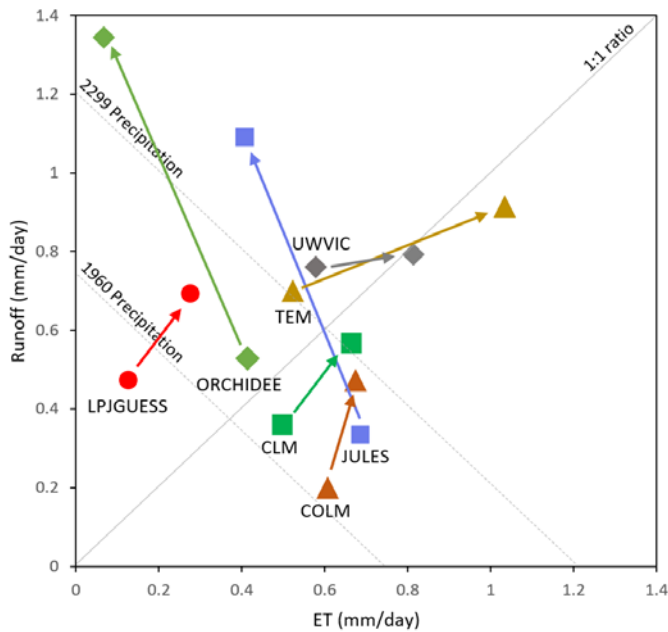
215

216 Models may project surface soil drying but the hydrological pathways through which this drying occurs
 217 appears to differ across models. The diversity of precipitation partitioning (Figure 5) demonstrates that
 218 specific representations and parameterizations for ET and runoff are not consistent across models. Though
 219 some models maintain a similar R/P ratio throughout the simulation (e.g., CLM, COLM, LPJGUESS),
 220 others show shifts from an ET-dominated system to a runoff-dominated system (e.g. JULES) and vice
 221 versa (e.g. TEM6 and UWWIC).

222 Evapotranspiration from the permafrost area is projected to rise in all models driven by warmer air
 223 temperatures and more productive vegetation, but the amplitude of that trend varies widely. The average
 224 projected evapotranspiration increase is 0.1 ± 0.1 mm/day by 2100, which represents about a 25% increase
 225 over 20th century levels. Beyond 2100, the ET projections diverge (Figure 2e).

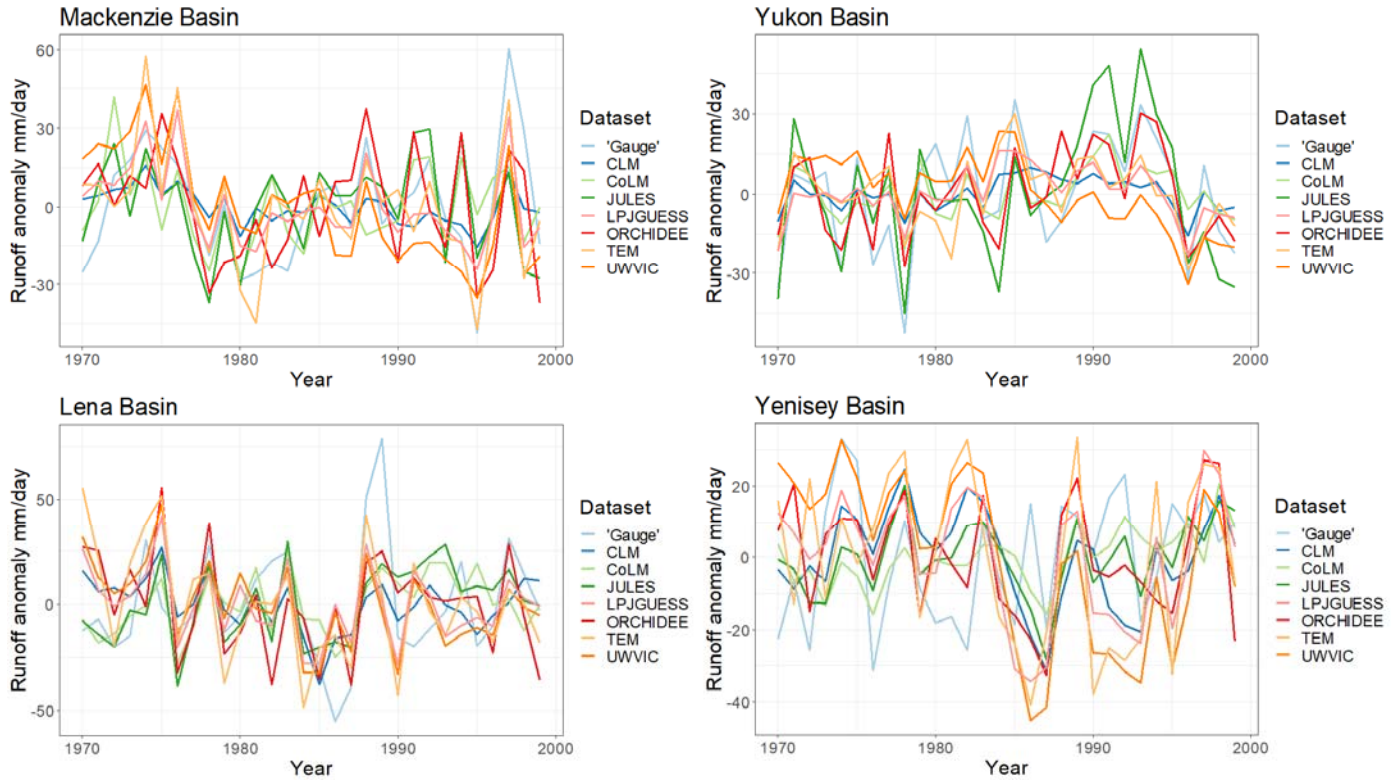
226 Runoff is also projected to increase with projections across models being highly variable (Figure 2g). The
 227 change in the models' ensemble mean between 1960-2299 was 0.2 ± 0.2 mm/day. CLM, COLM,
 228 LPJGUESS and TEM6 simulated runoff changes of 0.2 to 0.3 mm/day by 2299. UWWIC exhibit small to
 229 null changes in runoff while SIBCASA shows surface runoff only. JULES exhibited the highest runoff
 230 change with $+0.8$ mm/day for 2299, consistent with its high applied precipitation trend.

231 Comparison between gauge station data and runoff simulations from the major river basins in the
 232 permafrost region shows that most models agree on the long term timing (Figure 6, Table 3) but the
 233 magnitude is generally underestimated (Figure 7). The gauge discharge mean for the four river basins is
 234 219 ± 36 mm/yr compared to the models' ensemble mean of 101 ± 82 mm/yr for the period 1970-1999.
 235 Excluding SIBCASA, the models' ensemble mean is 134 ± 69 mm/yr. However, models show reasonable
 236 correlations between runoff output and observed annual discharge time series (Table 3). SIBCASA
 237 horizontal subsurface runoff was disabled on the simulation because it tended to drain the active layer
 238 completely, resulting in very low and unrealistic soil moisture. Therefore, SIBCASA runoff values shown
 239 in this study are only for surface runoff.
 240 The net water balance (P-ET-R) is projected to increase for most models with precipitation increases
 241 outpacing the sum of ET and runoff changes. All models except TEM6 show an increase in the net water
 242 balance over the simulation period which suggests that models are collecting soil water deeper in the soil
 243 column, presumably in response to increasing ALT, even while the top soil layers dry.
 244
 245



246
 247
 248 **Figure 5. Precipitation partitioning between total runoff and evapotranspiration for participating**
 249 **models. Markers and arrows indicate the change from initial period (1960-1989 average) to final**
 250 **period (2270-2299 average). Diagonal dashed lines represent the ensemble rainfall mean for the**
 251 **initial (0.74 mm/day) and final (1.2 mm/day) simulation years. At any point along the dashed**
 252 **diagonals, runoff and ET sum to precipitation.**

253
 254
 255

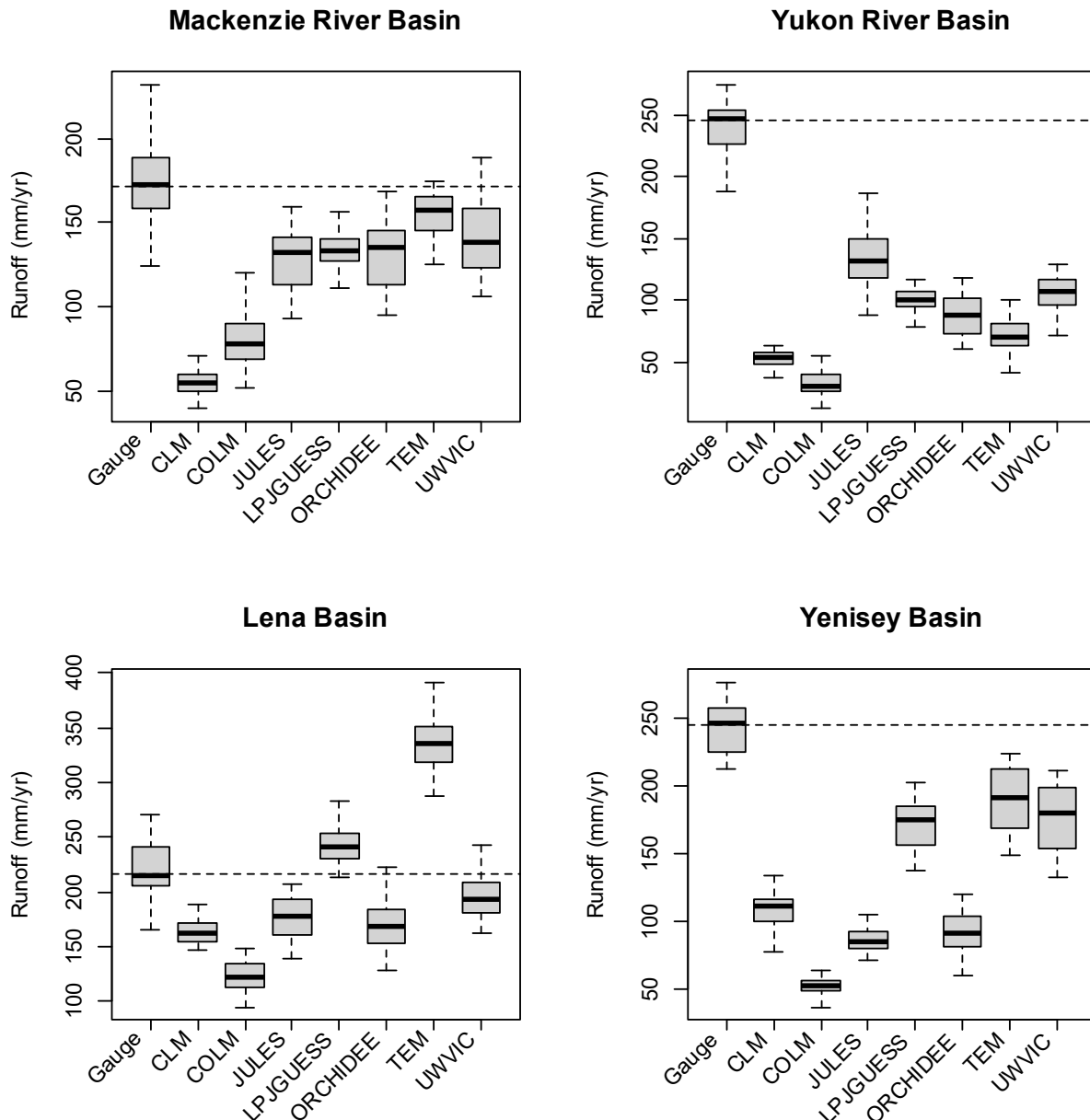


256
 257 **Figure 6. Runoff anomaly comparison between gauge data and models simulations for the period**
 258 **1970-1999 mean.**

259
 260 **Table 3. Correlation coefficients between simulated annual total runoff and gauge mean annual**
 261 **discharge 1970 to 1999. SIBCASA correlations are for surface runoff.**

Model	River Basin				Avg.
	Mackenzie	Yukon	Yenisey	Lena	
CLM	0.70	0.64	0.08	0.46	0.47
ORCHIDEE	0.57	0.69	0.36	0.37	0.50
LPJGUESS	0.68	0.71	0.14	0.35	0.47
TEM	0.66	0.56	0.16	0.40	0.45
SIBCASA	0.49	0.21	0.08	0.29	0.27
JULES	0.41	0.77	0.34	0.51	0.51
COLM	0.38	0.76	0.27	0.46	0.47
UWVIC	0.44	0.38	0.02	0.31	0.29
Avg.	0.54	0.59	0.18	0.40	

262



263
 264 **Figure 7. Discharge comparison between gauge station data and model output for each river basin.**
 265 **Dashed line indicates mean annual discharge at gauge station. Boxplots derived from mean annual**
 266 **discharge (total runoff) simulations for the period of 1970 to 1999.**

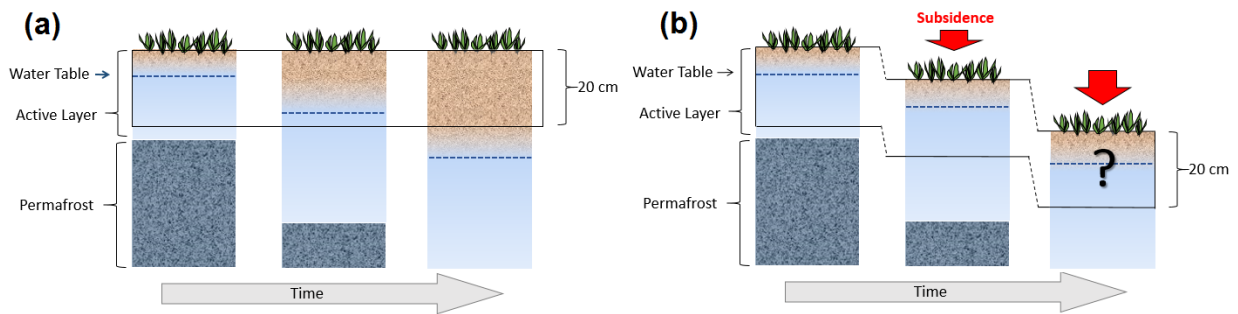
267
 268 **4. Discussion**

269
 270 This study assessed near-surface soil moisture and hydrology projections in the permafrost region using
 271 widely-used land models that represent permafrost. Most models showed near-surface drying despite the
 272 externally-forced intensification of the water cycle driven by climate change. Drying was generally
 273 associated with increases of active layer thickness and permafrost degradation in a warming climate. We
 274 show that the timing and magnitude of projected soil moisture changes vary widely across models,

275 pointing to an uncertain future in permafrost hydrology and associated climatic feedbacks. In this section,
 276 we review the role of projected permafrost loss and active layer thickening on soil moisture changes and
 277 some potential sources of variability among models. In addition, we comment on the potential effects of
 278 soil moisture projections on the permafrost carbon-climate feedback. It is important to note that this study
 279 is more qualitative in nature and does not focus on the detail of magnitude or spatial patterns of model
 280 signatures.

281
 282 **4.1 Permafrost degradation and drying**
 283

284 Increases in net precipitation and the counterintuitive drying of the top soil in the permafrost region
 285 suggests that soil column processes such as changes in active layer thickness (ALT) and activation of
 286 subsurface drainage with permafrost thaw are acting to dry the top soil layers (Figure 8a). In general,
 287 models represent impermeable soils when frozen. Then, as soils thaw at progressively depths in the
 288 summer, liquid water infiltrates further into the active layer draining deeper into the thawed soil column
 289 (Avis et al., 2011; Lawrence et al., 2015; Swenson et al., 2012). However, relevant soil column processes
 290 related to thermokarst by thawing of excess ground ice (Lee et al., 2014) are limited in these simulations
 291 despite their significant occurrence in the permafrost region (Olefeldt et al., 2016). As permafrost thaws,
 292 ground ice melts, potentially reducing the volume of the soil column and changing the hydrological
 293 properties of the soil (Aas et al., 2019; Nitzbon et al., 2019). This would occur where soil surface
 294 elevation drops through sudden collapse or slow deformation by an amount equal to or greater than the
 295 increased depth of annual thaw (Figure 8b). This mechanism, not represented in current large-scale
 296 models, could result in projected increases or no change in the water table over time as observed by long-
 297 term studies (Andresen and Loughheed, 2015; Mauritz et al., 2017; Natali et al., 2015). Subsidence of 12-
 298 13 cm has been observed in Northern Alaska over a five year period, which represents a volume loss of
 299 about 25% of the average ALT for that region (~50cm) (Streletskiy et al., 2008). These lines of evidence
 300 may suggest that permafrost thaw may not dry the Arctic as fast as simulated by land models but rather
 301 maintain or enhanced soil water saturation depending on the water balance of the modeled cell column.
 302



303
 304 **Figure 8. Schematic of changes in the soil column moisture (a) without subsidence (current models)**
 305 **and (b) with subsidence from thawing ice-rich permafrost (not represented by models), a process**
 306 **that may accumulate soil moisture and slow down drying over time.**
 307

308 Recent efforts have been made to address the high sub-grid heterogeneity of fine-scale mechanisms
 309 including soil subsidence (Aas et al., 2019), hillslope hydrology, talik and thermokarst development
 310 (Jafarov et al., 2018), ice wedge degradation (Abolt et al., 2018; Liljedahl et al., 2016; Nitzbon et al.,
 311 2019), vertical and lateral heat transfer on permafrost thaw and groundwater flow (Kurylyk et al., 2016)

312 and lateral water fluxes (Nitzbon et al., 2019). These processes are known to have a major role on surface
313 and subsurface hydrology and their implementation in large scale models is needed. Other important
314 challenges in land models' hydrology include representation of the significant area dynamics of the
315 ubiquitous smaller, shallow water bodies observed over recent decades (Andresen and Loughheed, 2015;
316 Jones et al., 2011; Roach et al., 2011; Smith et al., 2005). These systems are either lacking in simulations
317 (polygon ponds and small lakes) or assumed to be static systems in simulations (large lakes). The
318 implementation of surface hydrology dynamics and permafrost processes in large-scale land models will
319 help reduce uncertainty in our ability to predict the future hydrological state of the Arctic and the
320 associated climatic feedbacks. It is important to note that all these processes require data for model
321 calibration, verification and evaluation, that is commonly absent at large scales. Permafrost hydrology
322 will only advance through synergistic efforts between field researchers and modelers.

323

324 **4.2 Uncertainty in soil moisture and hydrology simulations**

325 Differences in representations of soil thermal dynamics can directly affect hydrology through timing of
326 the freezing-thawing cycle and by altering the rates of permafrost loss and subsurface drainage (Finney et
327 al., 2012). McGuire et al. (2016) and Peng et al. (2016) show that these models exhibit considerable
328 differences in permafrost quantities such as active layer thickness, and the mean and trends in near-
329 surface (0-3m) permafrost extent, even though all the models are forced with observed climatology.
330 However, these differences are smaller than those seen across the CMIP5 models (Koven et al., 2013). All
331 models except ORCHIDEE employ a multi-layer finite difference heat diffusion for soil thermal
332 dynamics (Table 2). Organic soil insulation, snow insulation, and unfrozen water effects on phase change
333 are the most common structural differences among models for soil thermal dynamics but do not explain
334 the variability in the simulated changes in ALT and permafrost area as shown by McGuire *et al* (2016).
335 Half of the participating models include organic matter in the soil properties (CLM, ORCHIDEE,
336 SIBCASA, UWVIC) which can significantly impact soil thermal properties and lead to an increase in the
337 hydraulic conductivity of the soil column, thereby enhancing drainage and redistribution of water in the
338 soil column. Soil vertical characterization is another important aspect for soil thermal dynamics and
339 hydrology (Chadburn et al., 2015; Nicolsky et al., 2007). Lawrence et al (2008) indicated that a high-
340 resolution soil column representation is necessary for accurate simulation of long term trends in active
341 layer depth. However, McGuire *et al* (2016) showed that soil column depth did not clearly explain
342 variability of the simulated loss of permafrost area across models.

343 Water table representation can result in a first order effect on soil moisture. Most models (CLM, COLM,
344 SIBCASA and ORCHIDEE) use some version of TOPMODEL (Niu et al., 2007), which employs a
345 prognostic water table where sub-grid scale topography is the main driver of soil moisture variability in
346 the cell. However, water table is not explicitly represented in other models such as LPJGUESS, which has
347 a uniform water table which is only applied for wetland areas. In addition to water table, storage and
348 transmission of water in soils is a fundamental component of an accurate representation of soil moisture
349 (Niu and Yang, 2006). The representation of soil water storage and transmission varies across models
350 from Richards equations based on Clapp Hornberger and/or van Genuchten (1980) functions (e.g CLM,
351 CoLM, SIBCASA, ORCHIDEE) to a simplified one layer bucket (e.g. TEM6). It is also important to
352 note that most models differ in their numerical implementations of processes, such as water movement
353 through frozen soils (Gouttevin, I. et al., 2012; Swenson et al., 2012), and in the use of iterative solutions
354 and vertical discretization of water transmission (De Rosnay et al., 2000).

355 Differences in representation of vertical fluxes through evapotranspiration (ET) are also likely adding to
356 the high variability in soil moisture projections. ET sources (e.g. interception loss, plant transpiration, soil
357 evaporation) were similar across models but had different formulations (Table 2). The diversity of ET
358 implementations (e.g. evaporative resistances from fractional areas, etc.) and of vegetation maps used by
359 the modelling groups (Ottlé et al., 2013) can also contribute to the big spread on the temporal simulations
360 for ET and soil moisture. Along with projected increases in ET, net precipitation (P-ET) is projected to
361 increase for all models suggesting that drying is not attributed only to soil evaporation, and the increasing
362 net water balance (P-ET-R) proposes that models are storing water deeper in the soil column as
363 permafrost near the surface thaws.

364 Despite runoff improvements (Swenson et al., 2012), underestimation of river discharge has been a
365 challenge in previous versions in models (Slater et al., 2007). The differences between models and
366 observations in mean annual discharge may stem from several sources. Particularly, the substantial
367 variation in the precipitation forcing for these models (Figure 2e). This is attributed, in part, to the sparse
368 observational networks in high latitudes. River discharge at high latitudes can differ substantially when
369 different reanalysis forcing datasets are used. For example, river discharge for Arctic rivers differs
370 substantially in CLM4.5 simulations when forced with GSWP3v1 compared to CRUNCEPv7 reanalysis
371 datasets (not shown, runoff for MacKenzie, +32%; Yukon, +78%; Lena, -2%; Yenisey, +22%). Other
372 factors include potential deficiencies in the parameterization and/or implementation of ET and runoff
373 processes as well as vegetation processes.

374

375 **4.3 Implications for the permafrost carbon-climate feedback**

376

377 If drying of the permafrost region occurs, carbon losses from the soil will be dominated by CO₂ as a result
378 of increased heterotrophic respiration rates compared to moist conditions (Elberling et al., 2013;
379 Oberbauer et al., 2007; Schädel et al., 2016). With projected drying, CH₄ flux emissions will slow down
380 by the reduction of soil saturation and inundated areas through lowering the water table in grid cells
381 (Figure 8A). In a sensitivity study using CLM, the slower increase of methane emissions associated with
382 surface drying could potentially lead to a reduction in the Global Warming Potential of permafrost carbon
383 emissions by up to 50% compared to saturated soils (Lawrence et al., 2015). However, we need to also
384 consider that current land models lack representation of important CH₄ sources and pathways in the
385 permafrost region such as lake and wetland dynamics that can counteract the suppression of CH₄ fluxes
386 by projected drying. Seasonal wetland area variation, which is not represented or is poorly represented in
387 current models, can contribute to a third of the annual CH₄ flux in boreal wetlands (Ringeval et al., 2012).
388 Although this manuscript may raise more questions than answers, this study highlights the importance of
389 advancing hydrology and hydrological heterogeneity in land models to help determine the spatial
390 variability, timing, and reasons for changes in hydrology of terrestrial landscapes of the Arctic. These
391 improvements may constrain projections of land-atmosphere carbon exchange and reduce uncertainty on
392 the timing and intensity of the permafrost carbon feedback.

393

394 **Data availability**

395

396 The simulation data analyzed in this manuscript is available through the National Snow and Ice Data
397 Center (NSIDC; <http://nsidc.org>). Inquires please contact Kevin Schaefer (kevin.schaefer@nsidc.org).

398

399 **Author contributions**

400
401 This manuscript is a collective effort of the modeling groups of the Permafrost Carbon Network
402 (<http://www.permafrostcarbon.org>). C.G.A, D.M.L., C.J.W., A.D.M. wrote the initial draft with additional
403 contributions of all authors. Figures prepared by C.G.A.
404

405 **Acknowledgements**

406
407 This manuscript is dedicated to the memory of Andrew G. Slater (1971 -2016) for his scientific
408 contributions in advancing Arctic hydrology modeling. This work was performed under the Next-
409 Generation Ecosystem Experiments (NGEE Arctic, DOE ERKP757) project supported by the Office of
410 Biological and Environmental Research in the U.S. Department of Energy, Office of Science. The study
411 was also supported by the National Science Foundation through the Research Coordination Network
412 (RCN) program and through the Study of Environmental Arctic Change (SEARCH) program in support
413 of the Permafrost Carbon Network. We also acknowledge the joint DECC/Defra Met Office Hadley
414 Centre Climate Programme (GA01101) and the European Union FP7-ENVIRONMENT project PAGE21.
415

416 **References**

417
418 Aas, K. S., Martin, L., Nitzbon, J., Langer, M., Boike, J., Lee, H., Berntsen, T. K. and Westermann, S.:
419 Thaw processes in ice-rich permafrost landscapes represented with laterally coupled tiles in a land surface
420 model, *Cryosphere*, 13(2), 591–609, doi:10.5194/tc-13-591-2019, 2019.
421 Abolt, C. J., Young, M. H., Atchley, A. L. and Harp, D. R.: Microtopographic control on the ground
422 thermal regime in ice wedge polygons, *Cryosphere*, 12(6), 1957–1968, doi:10.5194/tc-12-1957-2018,
423 2018.
424 Andresen, C. G. and Lougheed, V. L.: Disappearing arctic tundra ponds: Fine-scale analysis of surface
425 hydrology in drained thaw lake basins over a 65 year period (1948-2013)., *J. Geophys. Res.*, 120, 1–14,
426 doi:10.1002/2014JG002778, 2015.
427 Andresen, C. G., Lara, M. J., Tweedie, C. T. and Lougheed, V. L.: Rising plant-mediated methane
428 emissions from arctic wetlands, *Glob. Chang. Biol.*, 23(3), 1128–1139, doi:10.1111/gcb.13469, 2017.
429 Avis, C. a., Weaver, A. J. and Meissner, K. J.: Reduction in areal extent of high-latitude wetlands in
430 response to permafrost thaw, *Nat. Geosci.*, 4(7), 444–448, doi:10.1038/ngeo1160, 2011.
431 Best, M. J., Pryor, M., Clark, D. B., Rooney, G. G., Essery, R. L. H., Menard, C. B., Edwards, J. M.,
432 Hendry, M. a., Porson, a., Gedney, N., Mercado, L. M., Sitch, S., Blyth, E., Boucher, O., Cox, P. M.,
433 Grimmond, C. S. B. and Harding, R. J.: The Joint UK Land Environment Simulator (JULES), model
434 description. Part 1: Energy and water fluxes, *Geosci. Model Dev.*, 4, 677–699, doi:10.5194/gmdd-4-641-
435 2011, 2011.
436 Bohn, T. J., Podest, E., Schroeder, R., Pinto, N., McDonald, K. C., Glagolev, M., Filippov, I., Maksyutov,
437 S., Heimann, M., Chen, X. and Lettenmaier, D. P.: Modeling the large-scale effects of surface moisture
438 heterogeneity on wetland carbon fluxes in the West Siberian Lowland, *Biogeosciences*, 10(10), 6559–
439 6576, doi:10.5194/bg-10-6559-2013, 2013.
440 Bonan, G. B.: A Land Surface Model (LSM v1.0) for Ecological, Hydrological and Atmospheric studies:
441 Technical descripton and user’s guide., 1996.
442 Chadburn, S. E., Burke, E. J., Essery, R. L. H., Boike, J., Langer, M., Heikenfeld, M., Cox, P. M. and
443 Friedlingstein, P.: Impact of model developments on present and future simulations of permafrost in a
444 global land-surface model, *Cryosphere*, 9(4), 1505–1521, doi:10.5194/tc-9-1505-2015, 2015.
445 Dai, Y., Zeng, X., Dickinson, R. E., Baker, I., Bonan, G. B., Bosilovich, M. G., Denning, A. S., Dirmeyer
446 P, Houser, P. R., Niu, G., Oleson, K. W., Schlosser, C. A. and Yang, Z.: The Common Land Model

447 (CoLM), *Bull. Am. Meteorol. Soc.*, 84, 1013–1023, doi:10.1175/BAMS-84-8-1013, 2003.

448 Elberling, B., Michelsen, A., Schädel, C., Schuur, E. A. G., Christiansen, H. H., Berg, L., Tamstorf, M. P.
449 and Sigsgaard, C.: Long-term CO₂ production following permafrost thaw, *Nat. Clim. Chang.*, 3(October),
450 890–894, doi:10.1038/nclimate1955, 2013.

451 Finney, D. L., Blyth, E. and Ellis, R. .: Improved modelling of Siberian river flow through the use of an
452 alternative frozen soil hydrology scheme in a land surface model, *Cryosph.*, 6, 859–870,
453 doi:https://doi.org/10.5194/tc-6-859-2012, 2012.

454 Francini, M. and Paciani, M.: Comparative analysis of several conceptual rainfall-runoff models, *J.*
455 *Hydrol.*, 122, 161–219, 1991.

456 Frey, K. E. and McClelland, J. W.: Impacts of permafrost degradation on arctic river biogeochemistry,
457 *Hydrol. Process.*, 23, 169–182, doi:10.1002/hyp, 2009.

458 Gent, P. R., Danabasoglu, G., Donner, L. J., Holland, M. M., Hunke, E. C., Jayne, S. R., Lawrence, D.
459 M., Neale, R. B., Rasch, P. J., Vertenstein, M., Worley, P. H., Yang, Z. L. and Zhang, M.: The
460 community climate system model version 4, *J. Clim.*, 24(19), 4973–4991, doi:10.1175/2011JCLI4083.1,
461 2011.

462 Gerten, D., Schaphoff, S., Haberlandt, U., Lucht, W. and Sitch, S.: Terrestrial vegetation and water
463 balance — hydrological evaluation of a dynamic global vegetation model, , 286, 249–270,
464 doi:10.1016/j.jhydrol.2003.09.029, 2004.

465 Gouttevin, I., Krinner, G., Ciais, P., Polcher, J. and Legout, C.: Multi-scale validation of a new soil
466 freezing scheme for a land-surface model with physically-based hydrology, *Cryosph.*, 6, 407–430, 2012.

467 Grosse, G., Jones, B. and Arp, C.: Thermokarst lakes, drainage, and drained basins, in *Treatise on*
468 *Geomorphology*, vol. 8, pp. 325–353., 2013.

469 Harris, I., Jones, P. D., Osborn, T. J. and Lister, D. H.: Updated high-resolution grids of monthly climatic
470 observations - the CRU TS3.10 Dataset, *Int. J. Climatol.*, 34(3), 623–642, doi:10.1002/joc.3711, 2014.

471 Haxeltine, A. and Prentice, I. C.: A General Model for the Light-Use Efficiency of Primary Production,
472 *Funct. Ecol.*, 10(5), 551–561, 1996.

473 Hayes, D. J., McGuire, A. D., Kicklighter, D. W., Gurney, K. R., Burnside, T. J. and Melillo, J. M.: Is the
474 northern high - latitude land - based CO₂ sink weakening ?, *Global Biogeochem. Cycles*, 25(May), 1–14,
475 doi:10.1029/2010GB003813, 2011.

476 Hayes, D. J., Kicklighter, D. W., McGuire, a D., Chen, M., Zhuang, Q., Yuan, F., Melillo, J. M. and
477 Wullschleger, S. D.: The impacts of recent permafrost thaw on land–atmosphere greenhouse gas
478 exchange, *Environ. Res. Lett.*, 9(4), 045005, doi:10.1088/1748-9326/9/4/045005, 2014.

479 Jafarov, E. and Schaefer, K.: The importance of a surface organic layer in simulating permafrost thermal
480 and carbon dynamics, *Cryosph.*, 10, 465–475, doi:10.5194/tc-10-465-2016, 2016, 2016.

481 Jafarov, E. E., Coon, E. T., Harp, D. R., Wilson, C. J., Painter, S. L., Atchley, A. L. and Romanovsky, V.
482 E.: Modeling the role of preferential snow accumulation in through talik development and hillslope
483 groundwater flow in a transitional permafrost landscape, *Environ. Res. Lett.*, 13(10), doi:10.1088/1748-
484 9326/aadd30, 2018.

485 Jensen, M. E. and Haise, H. R.: Estimating evapotranspiration from solar radiation, *J. Irrig. Drain. Div.*
486 *ASCE*, (89), 15–41, 1963.

487 Ji, D., Wang, L., Feng, J., Wu, Q., Cheng, H., Q, Z., Yang, J., Dong, W., Dai, Y., Gong, D., Zhang, R. H.,
488 Wang, X., Liu, J., Moore, J. C., Chen, D. and Zhou, M.: Description and basic evaluation of Beijing
489 Normal University Earth system model (BNU-ESM) version 1, *Geosci. Model Dev.*, 7, 2039–2064, 2014.

490 Jones, B. M., Grosse, G., Arp, C. D., Jones, M. C., Walter Anthony, K. M. and Romanovsky, V. E.:
491 Modern thermokarst lake dynamics in the continuous permafrost zone, northern Seward Peninsula,
492 Alaska, *J. Geophys. Res.*, 116, G00M03, doi:10.1029/2011JG001666, 2011.

493 Kanevskiy, M., Shur, Y., Jorgenson, T., Brown, D. R. N., Moskalenko, N., Brown, J., Walker, D. A.,
494 Reynolds, M. K. and Buchhorn, M.: Degradation and stabilization of ice wedges: Implications for
495 assessing risk of thermokarst in northern Alaska, *Geomorphology*, 297, 20–42,
496 doi:10.1016/j.geomorph.2017.09.001, 2017.

497 Koven, C., Friedlingstein, P., Ciais, P., Khvorostyanov, D., Krinner, G. and Tarnocai, C.: On the

498 formation of high-latitude soil carbon stocks: Effects of cryoturbation and insulation by organic matter in
499 a land surface model, *Geophys. Res. Lett.*, 36(21), 1–5, doi:10.1029/2009GL040150, 2009.

500 Koven, C. D., Riley, W. J. and Stern, A.: Analysis of permafrost thermal dynamics and response to
501 climate change in the CMIP5 earth system models, *J. Clim.*, 26(6), 1877–1900, doi:10.1175/JCLI-D-12-
502 00228.1, 2013.

503 Koven, C. D., Lawrence, D. M. and Riley, W. J.: Permafrost carbon–climate feedback is sensitive to deep
504 soil carbon decomposability but not deep soil nitrogen dynamics, *Proc. Natl. Acad. Sci.*, 201415123,
505 doi:10.1073/pnas.1415123112, 2015.

506 Krinner, G., Viovy, N., de Noblet-Ducoudré, N., Ogée, J., Polcher, J., Friedlingstein, P., Ciais, P., Sitch,
507 S. and Prentice, I. C.: A dynamic global vegetation model for studies of the coupled atmosphere-
508 biosphere system, *Global Biogeochem. Cycles*, 19(1), 1–33, doi:10.1029/2003GB002199, 2005.

509 Kurylyk, B. L., Hayashi, M., Quinton, W. L., McKenzie, J. M. and Voss, C. I.: Influence of vertical and
510 lateral heat transfer on permafrost thaw, peatland landscape transition, and groundwater flow, *Water*
511 *Resour. Res.*, 52(2), 1286–1305, doi:10.1002/2015WR018057, 2016.

512 Lara, M. J., McGuire, A. D., Euskirchen, E. S., Tweedie, C. E., Hinkel, K. M., Skurikhin, A. N.,
513 Romanovsky, V. E., Grosse, G., Bolton, W. R. and Genet, H.: Polygonal tundra geomorphological change
514 in response to warming alters future CO₂ and CH₄ flux on the Barrow Peninsula, *Glob. Chang. Biol.*,
515 21, 1663–1651, doi:10.1111/gcb.12757, 2015.

516 Lawrence, D. M., Slater, A. G., Romanovsky, V. E. and Nicolsky, D. J.: Sensitivity of a model projection
517 of near-surface permafrost degradation to soil column depth and representation of soil organic matter, *J.*
518 *Geophys. Res.*, 113(F2), F02011, doi:10.1029/2007JF000883, 2008.

519 Lawrence, D. M., Koven, C. D., Swenson, S. C., Riley, W. J. and Slater, A. G.: Permafrost thaw and
520 resulting soil moisture changes regulate projected high-latitude CO₂ and CH₄ emissions, *Environ. Res.*
521 *Lett.*, 10(9), 094011, doi:10.1088/1748-9326/10/9/094011, 2015.

522 Lee, H., Swenson, S. C., Slater, A. G. and Lawrence, D. M.: Effects of excess ground ice on projections
523 of permafrost in a warming climate, *Environ. Res. Lett.*, 9(12), 124006, doi:10.1088/1748-
524 9326/9/12/124006, 2014.

525 Liang, X., Lettenmaier, D. P., Wood, E. F. and Burges, S.: A simple hydrologically based model of land
526 surface water and energy fluxes for general circulation models, *J. Geophys. Res.*, 99(D7), 14415–14418,
527 1994.

528 Liljedahl, A., Boike, J., Daanen, R. P., Fedorov, A. N., Frost, G. V., Grosse, G., Hinzman, L. D., Iijma,
529 Y., Jorgenson, J. C., Matveyeva, N., Necsoiu, M., Reynolds, M. K., Romanovsky, V., Schulla, J., Tape,
530 K. D., Walker, D. A., Wilson, C., Yabuki, H. and Zona, D.: Pan-Arctic ice-wedge degradation in warming
531 permafrost and influence on tundra hydrology, *Nat. Geosci.*, 9(April), 312–319, doi:10.1038/ngeo2674,
532 2016.

533 Mauritz, M., Bracho, R., Celis, G., Hutchings, J., Natali, S. M., Pegoraro, E., Salmon, V. G., Schädel, C.,
534 Webb, E. E. and Schuur, E. A. G.: Nonlinear CO₂ flux response to 7 years of experimentally induced
535 permafrost thaw, *Glob. Chang. Biol.*, 23(9), 3646–3666, doi:10.1111/gcb.13661, 2017.

536 McGuire, A. D., Lawrence, D. M., Koven, C., Clein, J. S., Burke, E., Chen, G., Jafarov, E., MacDougall,
537 A. H., Marchenko, S., Nicolsky, D., Peng, S., Rinke, A., Ciais, P., Gouttevin, I., Hayes, D. J., Ji, D.,
538 Krinner, G., Moore, J. C., Romanovsky, V., Schädel, C., Schaefer, K., Schuur, E. A. G. and Zhuang, Q.:
539 The Dependence of the Evolution of Carbon Dynamics in the Northern Permafrost Region on the
540 Trajectory of Climate Change, *Proc. Natl. Acad. Sci.*, 2018.

541 McGuire, D. A., Koven, C. D., Lawrence, D. M., Burke, E., Chen, G., Chen, X., Delire, C. and Jafarov,
542 E.: Variability in the sensitivity among model simulations of permafrost and carbon dynamics in the
543 permafrost region between 1960 and 2009, *Global Biogeochem. Cycles*, 1–23,
544 doi:10.1002/2016GB005405. Received, 2016.

545 Mitchell, T. D. and Jones, P. D.: An improved method of constructing a database of monthly climate
546 observations and associated high-resolution grids, *Int. J. Climatol.*, 25(6), 693–712, doi:10.1002/joc.1181,
547 2005.

548 Natali, S. M., Schuur, E. a G., Mauritz, M., Schade, J. D., Celis, G., Crummer, K. G., Johnston, C.,

549 Krapek, J., Pegoraro, E., Salmon, V. G. and Webb, E. E.: Permafrost thaw and soil moisture driving CO₂
550 and CH₄ release from upland tundra, *J. Geophys. Res. Biogeosciences*, 120, 525–537,
551 doi:10.1002/2014JG002872.Received, 2015.

552 Newman, B. D., Throckmorton, H. M., Graham, D. E., Gu, B., Hubbard, S. S., Liang, L., Wu, Y.,
553 Heikoop, J. M., Herndon, E. M., Phelps, T. J., Wilson, C. J. and Wulfschleger, S. D.: Microtopographic
554 and depth controls on active layer chemistry in Arctic polygonal ground, *Geophys. Res. Lett.*, 42(6),
555 1808–1817, doi:10.1002/2014GL062804, 2015.

556 Nicolsky, D. J., Romanovsky, V. E., Alexeev, V. A. and Lawrence, D. M.: Improved modeling of
557 permafrost dynamics in a GCM land-surface scheme, *Geophys. Res. Lett.*, 34,
558 doi:10.1029/2007GL029525, 2007.

559 Nitzbon, J., Langer, M., Westerman, S., Martin, L., Schanke Aas, K. and Boike, J.: Modelling the
560 degradation of ice-wedges in polygonal tundra under different hydrological conditions, *Cryosph.*, 13,
561 1089–1123, 2019.

562 Niu, G.-Y., Yang, Z.-L., Dickinson, R. E., Gulden, L. E. and Su, H.: Development of a simple
563 groundwater model for use in climate models and evaluation with Gravity Recovery and Climate
564 Experiment data, *J. Geophys. Res.*, 112(D7), D07103, doi:10.1029/2006JD007522, 2007.

565 Niu, G. and Yang, Z.: Effects of Frozen Soil on Snowmelt Runoff and Soil Water Storage at a
566 Continental Scale, *J. Hydrometeorol.*, 7, 937–952, doi:10.1175/JHM538.1, 2006.

567 Oberbauer, S., Tweedie, C., Welker, J. M., Fahnestock, J. T., Henry, G. H. R., Webber, P. J., Hollister, R.
568 D., Walker, D. A., Kuchy, A., Elmore, E. and Starr, G.: Tundra CO₂ fluxes in response to experimental
569 warming across latitudinal and moisture gradients, *Ecol. ...*, 77(2), 221–238 [online] Available from:
570 <http://www.esajournals.org/doi/abs/10.1890/06-0649> (Accessed 10 July 2014), 2007.

571 Olefeldt, D., Goswami, S., Grosse, G., Hayes, D., Hugelius, G., Kuhry, P., McGuire, A. D., Romanovsky,
572 V. E., Sannel, A. B. K., Schuur, E. A. G. and Turetsky, M. R.: Circumpolar distribution and carbon
573 storage of thermokarst landscapes, *Nat. Commun.*, 7, 1–11, doi:10.1038/ncomms13043, 2016.

574 Oleson, K., Lawrence, D., Bonan, G., Drewniak, B., Huang, M., Koven, C., Levis, S., Li, F., Riley, W.,
575 Subin, Z., Swenson, S., Thornton, P., Bozbiyik, A., Fisher, R., Heald, C., Kluzek, E., Lamarque, J.-F.,
576 Lawrence, P., Leung, L., Lipscomb, W., Muszala, S., Ricciuto, D., Sacks, W., Sun, Y., Tang, J. and Yang,
577 Z.-L.: Technical description of version 4.5 of the Community Land Model (CLM), Boulder, Colorado.
578 [online] Available from: <http://opensky.library.ucar.edu/collections/TECH-NOTE-000-000-000-870>,
579 2013.

580 Ottlé, C., Lescure, J., Maignan, F., Poulter, B., Wang, T. and Delbart, N.: Use of various remote sensing
581 land cover products for plant functional type mapping over Siberia., *Earth Syst. Sci. Data*, 5(2), 331,
582 2013.

583 Peng, S., Ciais, P., Krinner, G., Wang, T., Gouttevin, I., McGuire, A. D., Lawrence, D., Burke, E., Chen,
584 X., Delire, C., Koven, C., MacDougall, A., Rinke, A., Saito, K., Zhang, W., Alkama, R., Bohn, T. J.,
585 Decharme, B., Hajima, T., Ji, D., Lettenmaier, D. P., Miller, P. A., Moore, J. C., Smith, B. and Sueyoshi,
586 T.: Simulated high-latitude soil thermal dynamics during the past four decades, *Cryosph. Discuss.*, 9(2),
587 2301–2337, doi:10.5194/tcd-9-2301-2015, 2015.

588 Rawlins, M. a., Steele, M., Holland, M. M., Adam, J. C., Cherry, J. E., Francis, J. a., Groisman, P. Y.,
589 Hinzman, L. D., Huntington, T. G., Kane, D. L., Kimball, J. S., Kwok, R., Lammers, R. B., Lee, C. M.,
590 Lettenmaier, D. P., McDonald, K. C., Podest, E., Pundsack, J. W., Rudels, B., Serreze, M. C.,
591 Shiklomanov, A., Skagseth, Ø., Troy, T. J., Vörösmarty, C. J., Wenshanan, M., Wood, E. F., Woodgate,
592 R., Yang, D., Zhang, K. and Zhang, T.: Analysis of the Arctic System for Freshwater Cycle
593 Intensification: Observations and Expectations, *J. Clim.*, 23(21), 5715–5737,
594 doi:10.1175/2010JCLI3421.1, 2010.

595 Ringeval, B., Decharme, B., Piao, S. L., Ciais, P., Papa, F., De Noblet-Ducoudré, N., Prigent, C.,
596 Friedlingstein, P., Gouttevin, I., Koven, C. and Ducharne, a.: Modelling sub-grid wetland in the
597 ORCHIDEE global land surface model: Evaluation against river discharges and remotely sensed data,
598 *Geosci. Model Dev.*, 5, 941–962, doi:10.5194/gmd-5-941-2012, 2012.

599 Roach, J., Griffith, B., Verbyla, D. and Jones, J.: Mechanisms influencing changes in lake area in Alaskan

600 boreal forest, *Glob. Chang. Biol.*, 17(8), 2567–2583, doi:10.1111/j.1365-2486.2011.02446.x, 2011.

601 De Rosnay, P. and Polcher, J.: Modelling root water uptake in a complex land surface scheme coupled to
602 a GCM, *Hydrol. Earth Syst. Sci.*, 2(2/3), 239–255, doi:10.5194/hess-2-239-1998, 1998.

603 De Rosnay, P., Bruen, M. and Polcher, J.: Sensitivity of surface fluxes to the number of layers in the soil
604 model used in GCMs, *Geophys. Res. Lett.*, 27(20), 3329–3332, doi:10.1029/2000GL011574, 2000.

605 Schädel, C., Bader, M. K.-F., Schuur, E. A. G., Biasi, C., Bracho, R., Čapek, P., De Baets, S., Diáková,
606 K., Ernakovich, J., Estop-Aragones, C., Graham, D. E., Hartley, I. P., Iversen, C. M., Kane, E.,
607 Knoblauch, C., Lupascu, M., Martikainen, P. J., Natali, S. M., Norby, R. J., O’Donnell, J. A., Chowdhury,
608 T. R., Šantrůčková, H., Shaver, G., Sloan, V. L., Treat, C. C., Turetsky, M. R., Waldrop, M. P. and
609 Wickland, K. P.: Potential carbon emissions dominated by carbon dioxide from thawed permafrost soils,
610 *Nat. Clim. Chang.*, 6(10), 950–953, doi:10.1038/nclimate3054, 2016.

611 Schaefer, K., Zhang, T., Bruhwiler, L. and Barrett, A. P.: Amount and timing of permafrost carbon
612 release in response to climate warming, *Tellus, Ser. B Chem. Phys. Meteorol.*, 63(2), 165–180,
613 doi:10.1111/j.1600-0889.2011.00527.x, 2011.

614 Sheffield, J., Goteti, G. and Wood, E. F.: Development of a 50-year high-resolution global dataset of
615 meteorological forcings for land surface modeling, *J. Clim.*, 19(13), 3088–3111, doi:10.1175/JCLI3790.1,
616 2006.

617 Slater, A. G. and Lawrence, D. M.: Diagnosing present and future permafrost from climate models, *J.*
618 *Clim.*, 26(15), 5608–5623, doi:10.1175/JCLI-D-12-00341.1, 2013.

619 Slater, A. G., Bohn, T. J., McCreight, J. L., Serreze, M. C. and Lettenmaier, D. P.: A multimodel
620 simulation of pan-Arctic hydrology, *J. Geophys. Res. Biogeosciences*, 112(4), 1–17,
621 doi:10.1029/2006JG000303, 2007.

622 Smith, L. C., Sheng, Y., MacDonald, G. M. and Hinzman, L. D.: Disappearing Arctic lakes., *Science*,
623 308(5727), 1429, doi:10.1126/science.1108142, 2005.

624 Streletskiy, D. A., Shiklomanov, N. I., Nelson, F. E. and Klene, A. E.: 13 Years of Observations at
625 Alaskan CALM Sites : Long-term Active Layer and Ground Surface Temperature Trends, in Ninth
626 International Conference on Permafrost, edited by D. L. Kane and K. M. Hinkel, pp. 1727–1732,
627 University of Alaska at Fairbanks, Fairbanks, AK., 2008.

628 Swenson, S. C., Lawrence, D. M. and Lee, H.: Improved simulation of the terrestrial hydrological cycle in
629 permafrost regions by the Community Land Model, *J. Adv. Model. Earth Syst.*, 4(8), 1–15,
630 doi:10.1029/2012MS000165, 2012.

631 Thornthwaite, C. and Mather, J. R.: Instructions and tables for computing potential evapotranspiration
632 and the water balance: Centeron, N.J., Laboratory of Climatology., *Publ. Climatol.*, 10(3), 185–311, 1957.

633 Throckmorton, H. M., Heikoop, J. M., Newman, B. D., Altmann, G. L., Conrad, M. S., Muss, J. D.,
634 Perkins, G. B., Smith, L. J., Torn, M. S., Wullschleger, S. D. and Wilson, C. J.: Pathways and
635 transformations of dissolved methane and dissolved inorganic carbon in Arctic tundra watersheds:
636 Evidence from analysis of stable isotopes, *Global Biogeochem. Cycles*, 29, 1893–1910,
637 doi:10.1002/2014GB005044.Received, 2015.

638 Walvoord, M. A. and Kurylyk, B. L.: Hydrologic Impacts of Thawing Permafrost—A Review, *Vadose*
639 *Zo. J.*, 15(6), 0, doi:10.2136/vzj2016.01.0010, 2016.

640 Wang, W., Rinke, A., Moore, J. C., Ji, D., Cui, X., Peng, S., Lawrence, D. M., McGuire, A. D., Burke, E.
641 J., Chen, X., Decharme, B., Koven, C., MacDougall, A., Saito, K., Zhang, W., Alkama, R., Bohn, T. J.,
642 Ciais, P., Delire, C., Gouttevin, I., Hajima, T., Krinner, G., Lettenmaier, D. P., Miller, P. A., Smith, B.,
643 Sueyoshi, T. and Sherstiukov, A. B.: Evaluation of air-soil temperature relationships simulated by land
644 surface models during winter across the permafrost region, *Cryosphere*, 10(4), 1721–1737,
645 doi:10.5194/tc-10-1721-2016, 2016.

646 Wania, R., Ross, I. and Prentice, I. C.: Integrating peatlands and permafrost into a dynamic global
647 vegetation model : 1 . Evaluation and sensitivity of physical land surface processes, , 23, 1–19,
648 doi:10.1029/2008GB003412, 2009a.

649 Wania, R., Ross, I. and Prentice, I. C.: Integrating peatlands and permafrost into a dynamic global
650 vegetation model : 2 . Evaluation and sensitivity of vegetation and carbon cycle processes, , 23, 1–15,

651 doi:10.1029/2008GB003413, 2009b.
652 Willmott, C. J. and Matsuura, K.: Terrestrial air temperature and precipitation: Monthly and annual time
653 series (1950–1999) Version 1.02., 2001.
654
655